

Published in IET Electric Power Applications
 Received on 16th April 2009
 Revised on 24th June 2009
 doi: 10.1049/iet-epa.2009.0086



Application of planar modular windings to linear induction motors by harmonic cancellation

*J.F. Eastham*¹ *T. Cox*² *J. Proverbs*²

¹The University of Bath, Bath BA2 7AY, UK

²Force Engineering Ltd, Shephed LE12 9NJ, UK

E-mail: thomas_d_cox@yahoo.co.uk

Abstract: The magnetomotive force (mmf) of a modular planar winding contains multiple distinct waveforms which travel in opposite directions. An inductive rotor will produce oppositional forces from both waveforms, giving a poor overall performance. This study concerns the use of planar modular windings in linear induction motors by harmonic cancellation. A double-sided arrangement of stators is used and a mechanical offset is applied between the two stators such that the fundamental mmf waveform is reinforced and the oppositional harmonic mmf waveform is suppressed. A comprehensive mathematical analysis of mmf harmonic behaviour in the offset machines has been developed. Further, a high-speed dynamic test rig has been produced, which verifies the excellent performance of the offset modular configuration.

1 Introduction

Windings that are known as concentrated or modular [1] are in use principally for permanent magnet machines and use coils that all occupy the same plane Fig. 1*a* and have a winding sequence *a b c*. They will be referred to as planar modular windings in this paper. Each coil in Fig. 1*a* may be replaced by a concentric group as shown in Fig. 1*b*. This reduces the end-turn leakage reactance which may be an advantage in some cases [2].

Planar concentrated windings have constructional simplicity compared with double-layer windings, and because the coils can be preformed without the need for complex end turn geometry the copper fill factor in the slots can be improved by a factor of the order of 50% when compared to the use of mush wound coils. A further advantage accrues when they are used as modules for long stator machines; unlike modules using double-layer windings they can be butted closely together to provide an array with constant current loading. Long stator short-rotor machines are becoming of increasing importance for unmanned aerial vehicle (UAV), aircraft and leisure ride launch.

The use of the windings for linear induction motors has been described in a number of publications. These may be divided into machines using wound rotors [3–6] and machines using offset stators [7–9]. In each of these papers only windings with a single coil in each group were considered.

A planar modular winding produces multiple distinct mmf waveforms, travelling in opposite directions. Both the wound rotor method and the offset stator method have been developed to suppress the effects of harmonics, leading to excellent performance from inductive rotors with simple planar modular stators. The dual coil concentric group winding has the same broad harmonic response as the winding with a single coil in a group and the same harmonic suppression techniques can be used.

The objective of this paper is to analyse and model the behaviour of the various mmf harmonics, including the effects of offsetting for both single and two coil group windings. Further, the positive effects of offset machines will be demonstrated using a high-speed dynamic test rig.

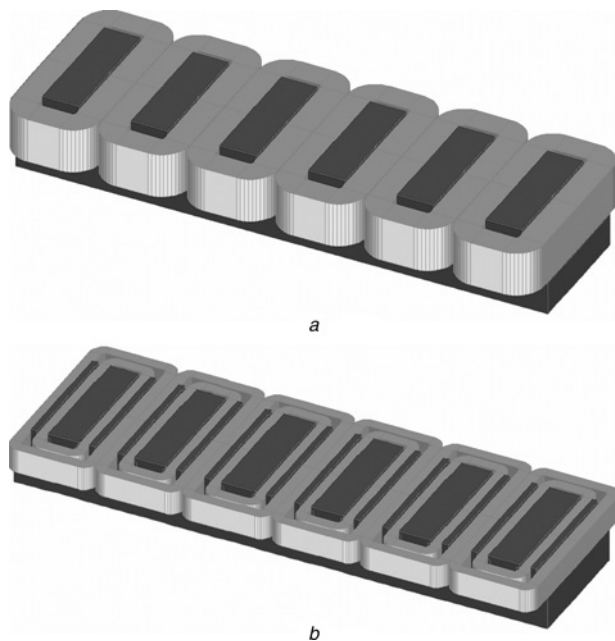


Figure 1 Modular winding stator

a Single coil in each group

b Two concentric coils in each group

2 Planar modular winding analysis

The planar modular windings that are most apt for use in linear induction motors are the three coil 2/4 pole, the nine coil 8/10 pole and the 12 coil 10/14 pole. The winding connections for these are given in Tables 1–3. It will be appreciated that each of these coil sequences can be repeated as many times as required.

The winding connections for windings using concentric groups as shown in Fig. 1*b* follow the same sequences as those given above.

Table 1 Three coil 2/4 pole modular winding connections

Coil number	1	2	3
coil phase and connection	<i>a</i>	<i>b</i>	<i>c</i>

Table 2 Nine coil 8/10 pole modular winding connections

Coil Number	1	2	3	4	5	6	7	8	9
coil phase and connection	<i>a</i>	$-a$	<i>a</i>	<i>b</i>	$-b$	<i>b</i>	<i>c</i>	$-c$	<i>c</i>

Table 3 Twelve coil 10/14 pole modular winding connections

Coil number	1	2	3	4	5	6	7	8	9	10	11	12
coil phase and connection	<i>a</i>	$-a$	$-b$	<i>b</i>	<i>c</i>	$-c$	$-a$	<i>a</i>	<i>b</i>	$-b$	$-c$	<i>c</i>

The winding distributions of a three-phase winding may be represented by positive, negative and zero-phase sequence sets each having three balanced windings. The harmonic numbers at which these sequence sets are present together with the harmonic winding factors k_{wp} are given below and are derived by the method detailed in Appendix for the example of a nine coil 8/10 pole winding.

When the windings are fed with a balanced set of currents a positive going field is produced by the forward sequence set and a negative going field is produced by the negative sequence set, no field is produced by the zero sequence set. It will be assumed that the supply is balanced and therefore that there is no zero sequence field in this paper.

2.1 Three coil 2/4 pole

$$k_{wp} = |\sin p\pi/3| \quad (1)$$

Positive sequence winding sets (PPS) at $p = 1, 4, 7, \dots$

Negative sequence winding sets (NPS) at $p = 2, 5, 8, \dots$

Table 4 shows the winding factors.

2.2 Nine coil 8/10 pole

$$k_{wp} = |\sin(\pi p/9)[2 \cos(2\pi p/9) - 1]| \quad (2)$$

Positive sequence winding sets (PPS) at $p = 1, 4, 7, \dots$

Negative sequence winding sets (NPS) at $p = 2, 5, 8, \dots$

Table 5 shows the winding factors.

2.3 Dual coil nine concentric group 8/10 pole

$$k_{wp} = |[2 \cos(2\pi p/9) - 1][\sin(\pi p/9) + \sin(k\pi p/9)]| \quad (3)$$

Positive sequence winding sets (PPS) at $p = 1, 4, 7, \dots$

Table 4 Three coil 2/4 pole amplitudes of winding sequence sets

	1	2	3	4	5	6
PPS	0.866	0	0	0.866	0	0
NPS	0	0.866	0	0	0.866	0

Table 5 Nine coil 8/10 pole amplitudes of winding sequence sets

	1	2	3	4	5	6
PPS	0.061	0	0	0.945	0	0
NPS	0	0.139	0	0	0.945	0
	7	8	9	10	11	12
PPS	0.139	0	0	0.061	0	0
NPS	0	0.061	0	0	0.139	0

Table 6 Dual coil nine concentric group 8/10 pole amplitudes of winding sequence sets

	1	2	3	4	5	6
PPS	0.0475	0	0	0.809	0	0
NPS	0	0.111	0	0	0.8695	0
	7	8	9	10	11	12
PPS	0.1764	0	0	0.0521	0	0
NPS	0	0.119	0	0	0.0214	0

Table 7 Twelve coil 10/14 pole amplitudes of winding sequence sets

	1	2	3	4	5	6	7
PPS	0	0	0	0	0.933	0	0
NPS	0.066	0	0	0	0	0	0.933
	8	9	10	11	12	13	
PPS	0	0	0	0.066	0	0	
NPS	0	0	0	0	0	0.066	

Negative sequence winding sets (NPS) at $p = 2, 5, 8, \dots$ where k is the ratio of the inner to the outer coil pitch in the group. The test machine used on the dynamic test rig described in Section 5 had a ratio of $k = 0.558$ and the winding factors in the case are as shown in Table 6.

2.4 Twelve coil 10/14 pole

$$k_{wp} = |\sin^2(\pi p/2)| \quad (4)$$

Positive sequence winding sets (PPS) at $p = 1, 7, 13, \dots$

Negative sequence winding sets (NPS) at $p = 5, 11, \dots$

Table 7 shows the winding factors.

From the tables it can be deduced that when energised with balanced three-phase currents all the windings will produce dominant fields that travel in opposite directions and would give oppositely directed forces on an induction machine secondary. In order to work successfully with a simple conductive sheet rotor, the dominant field travelling in one direction must be cancelled.

3 Principle of harmonic cancellation

The concept of harmonic cancellation is relatively simple. If the simplest case of a double-sided three coil section of a three coil 2/4 pole planar modular machine is considered, the two and four pole mmf waveform components can be drawn as in Fig. 2.

As would be expected, both the two pole forwards going and four pole backwards going waveforms reinforce. The overall mmf still contains both two and four pole components at double the magnitude of a single stator's components.

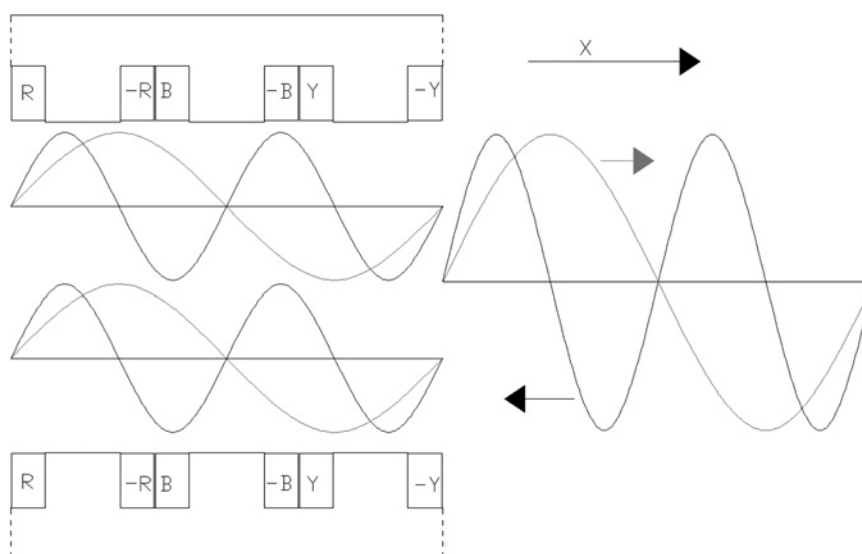


Figure 2 Two and four pole flux components from double-sided concentrated winding

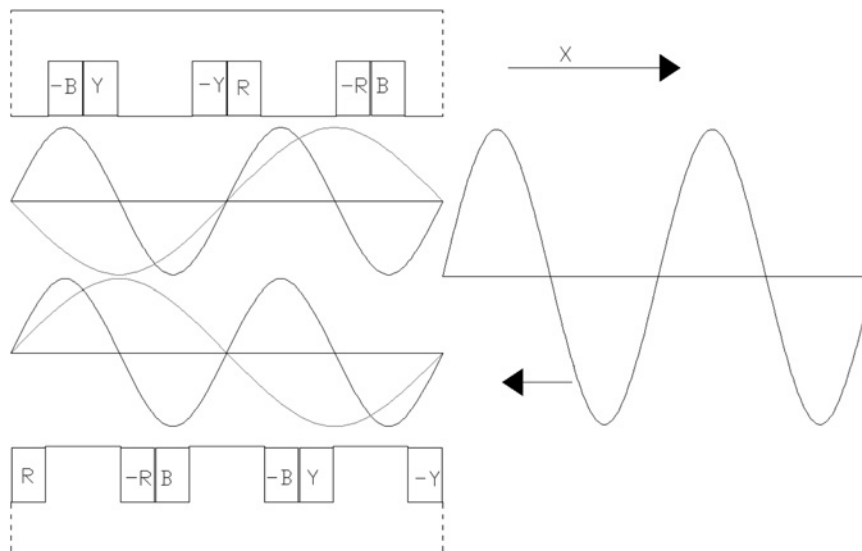


Figure 3 Flux components from offset double-sided concentrated winding, two pole cancellation

To improve this situation, a mechanical offset is introduced, displacing one stator in the direction of field travel (X in Fig. 2) relative to the other. An offset of 180° or one pole pitch of the two pole mmf wave produces the following flux pattern (Fig. 3).

It can be observed that total cancellation of the two pole mmf wave has occurred, leaving only the fully reinforced four pole mmf wave. A further modification is to reverse the polarity of the coils in one stator (Fig. 4).

As can be seen, reversing the polarity of one stator causes the four pole wave to be fully cancelled, and the two pole wave to be fully reinforced. This is an important result as it shows that the offset system can be used to produce either of the harmonics present, and totally suppress the other. Machines using this configuration of one reversed stator

will be referred to as reversed, for example six coil 4/8 pole reversed.

4 Double-sided offset stator behaviour

A double-sided linear machine uses a plate secondary that is sandwiched between two stators. If the windings of the stators are offset with respect to each other then the harmonic content of the total field can be modified. This gives the opportunity to cancel one of the dominant fields from planar non-overlapping windings so that force is produced substantially only in one direction and a viable system results.

Appendix shows that the amplitude of the phase sequence distribution from the pair of windings is multiplied by

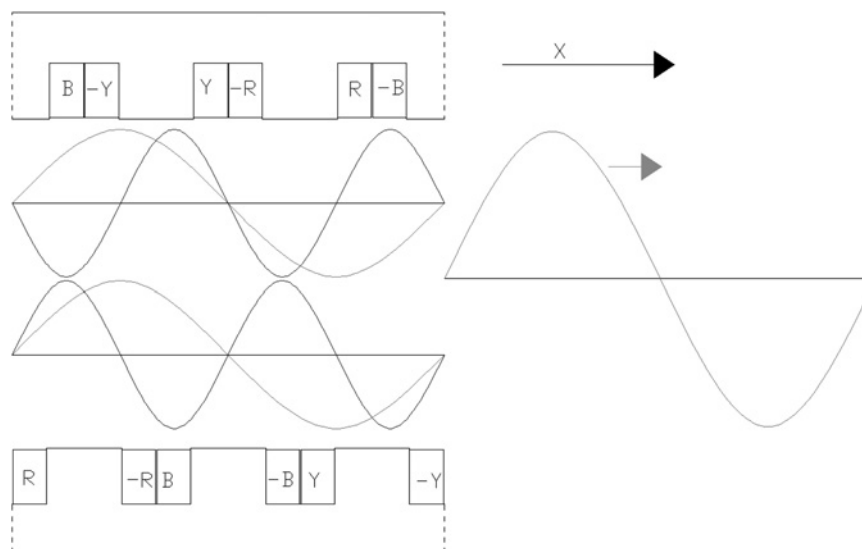


Figure 4 Flux components from offset double-sided concentrated winding, four pole cancellation

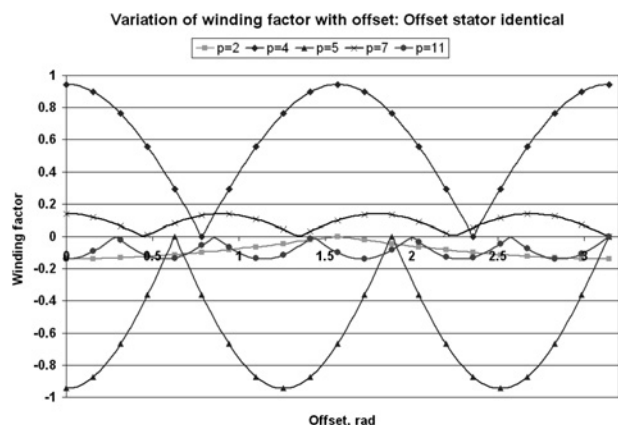


Figure 5 Winding factors for offset stators: offset winding identical

$|\cos \alpha p/2|$ when the offset winding is identical to the first winding and $|\sin \alpha p/2|$ when the offset winding is reversed.

Figs. 5 and 6 illustrate the effect using the nine slot 8/10 pole as an example, by showing the resulting winding factors at a range of offset positions. In Fig. 5 the offset winding is identical and in Fig. 6 it is reversed.

It can be seen that in the case of identical stators the fifth harmonic (ten poles) is cancelled at three overlap positions when

$$\left[\cos \frac{5\alpha}{2} \right] = 0 \quad \text{these are given by } \alpha = \frac{k\pi}{5} \quad \text{where } k = 1, 3, 5 \quad (5)$$

The winding factor of the wanted harmonic that is, $p = 4$ (eight poles) is different at these points and it is evident from Fig. 5 that putting $\alpha = \pi$ maximises the winding factor with full reinforcement of the eight pole wave. Table 8 shows the resulting harmonics.

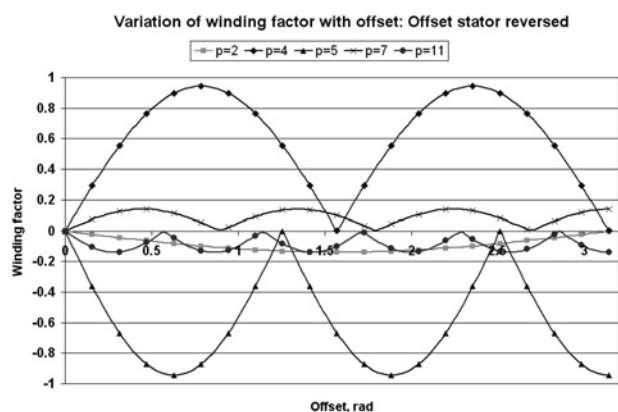


Figure 6 Winding factors for offset stators: offset winding reversed

Table 8 Nine coil 8/10 pole sequence array used for a π offset machine with identical windings. Amplitudes of winding sequence sets

	1	2	3	4	5	6
PPS	0	0	0	0.945	0	0
NPS	0	0.139	0	0	0	0
	7	8	9	10	11	12
PPS	0	0	0	0.061	0	0
NPS	0	0.061	0	0	0	0

Fig. 6 shows the winding factor for different offsets when the second winding is reversed. Here the $p = 4$ (eight pole) harmonic is zero when

$$\left[\sin \frac{4\alpha}{2} \right] = 0 \quad \text{this occurs when } \alpha = \frac{k\pi}{2} \quad \text{where } k = 1, 2 \quad (6)$$

When $\alpha = \pi/2$ the $p = 5$ winding factor is less than when $\alpha = \pi$ where the fields fully reinforce. $\alpha = \pi$ is therefore again the preferred offset. Table 9 shows the resulting harmonics.

Finite element analysis has been undertaken using the MEGA finite element (FE) package [10]. Airgap flux was analysed for a 2D representation of the nine coil 8/10 pole offset configuration described above firstly with no offset (Fig. 7a) and secondly with π offset (Fig. 7b). It can be seen that cancellation of the ten pole harmonic is achieved when using the π offset.

5 Dynamic test rig

In order to confirm the excellent performance of offset machines a full dynamic test rig has been developed, as shown in Fig. 8. The configuration is based on a high-speed linear launch machine. A rotating rig was used as this removes the need for a long track of stators while giving results close to those for a linear system.

Table 9 Nine coil 8/10 pole sequence array used for a π offset machine with one winding reversed. Amplitudes of winding sequence sets

	1	2	3	4	5	6
PPS	0.061	0	0	0	0	0
NPS	0	0	0	0	0.945	0
	7	8	9	10	11	12
PPS	0.139	0	0	0	0	0
NPS	0	0	0	0	0.139	0

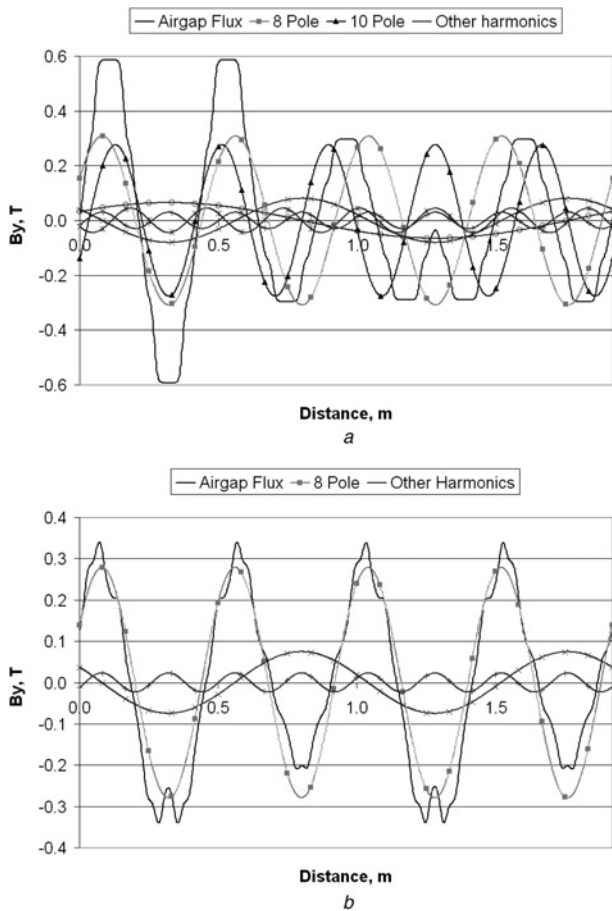


Figure 7 Airgap flux for double-sided pair of stators

a With no offset
b With π offset

This rig models a long stator short rotor machine and uses two full ring offset stators. Two aluminium rotor plates each six poles long are used. They are in diametrically opposed

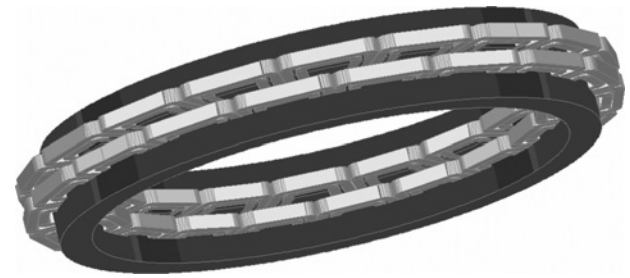


Figure 9 3D FE model of dynamic test rig stator

positions to aid mechanical balance. The windings are of the nine concentric group 8/10 pole configuration and have two coils per group as described in Section 3.3. The winding sequence is repeated twice and the stators are offset to cancel the ten pole harmonic via the methods outlined above. The cradle has been designed to rotate freely on the same axis as the rotor, via bearings. The cradle is linked to the frame by a force transducer as shown in Fig. 8, in order to measure the true force developed between the stators and the rotor. A load motor is attached to the rotor via a pulley system, with a rotary encoder to provide speed feedback. The test rig was designed to maintain the rotors at a required velocity using the load motor and measure the force developed by the test motors, as well as the power supply characteristics to the motors.

The results from the test rig were compared to a time stepped full three-dimensional (3D) finite element model based on the test rig design, with coupled external circuits [11] used to model the correct stator supply and resistance characteristics, based on rig measurements. The stator of this model is shown in Fig. 9. The model used two Lagrange surfaces [12] in the airgap, one on each side of the rotor conductor in order to allow the rotor mesh to

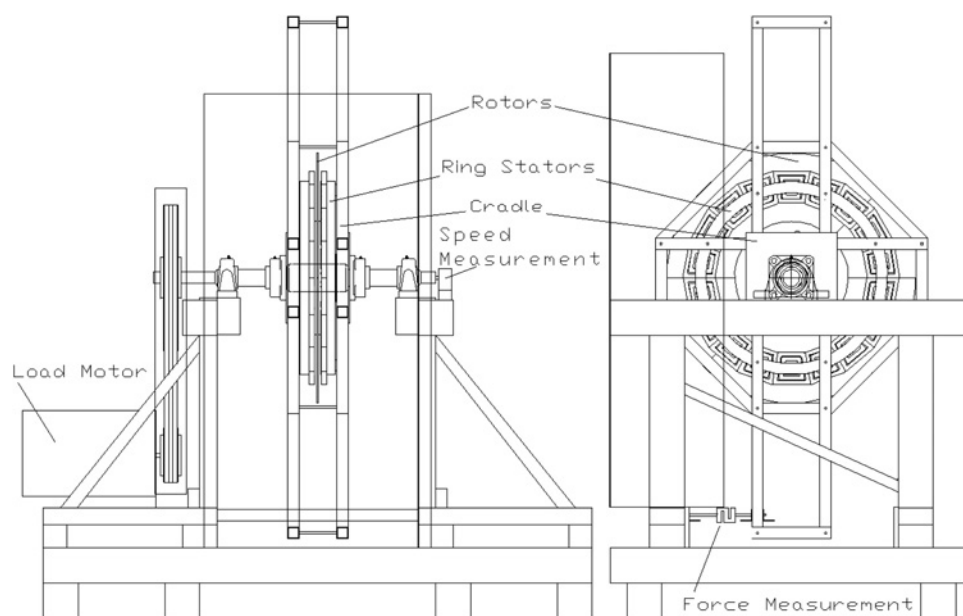


Figure 8 Nine coil 8/10 pole dynamic test rig

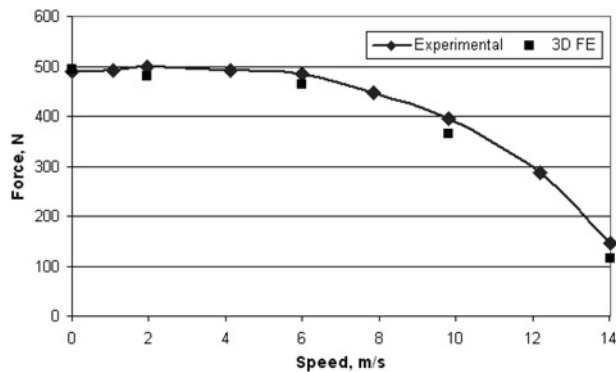


Figure 10 Force output at test rig current

move independently of the stator mesh without re-meshing. The finite element modelling was developed to be as close as possible to the test rig design, in order to model some of the effects present in the rotary rig that would not be present in a linear track. In particular, the rotor current paths will be affected, as they will be more constrained on the inside edge of the ring stator when compared to the outside edge. This effect will be accurately modelled with the full 3D FE model.

The results of the offset test rig modelling are shown below. Fig. 10 shows force output, Fig. 11 shows test rig current draw and Fig. 12 shows volt amperes per Newton (VA/N).

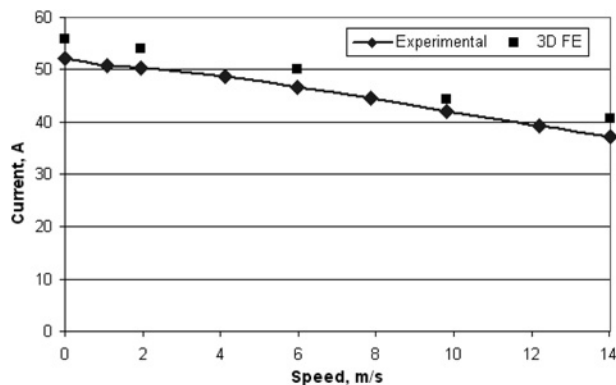


Figure 11 Input current at 400 V line

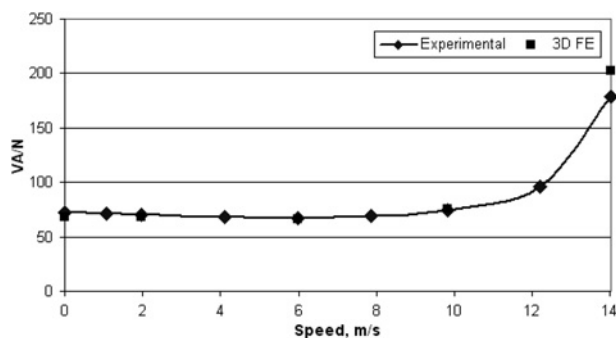


Figure 12 VA/N of test rig and 3DFE

6 Conclusions

The results above show excellent correlation with the FE modelling. Force and current from the test rig are close to FE modelled results, and VA/N is extremely close over the majority of the speed range. The offset concentrated machines will perform very well in high-speed launch applications, as has previously been predicted by FE [7, 8].

A method has also been demonstrated that gives accurate and comprehensive analysis of the mmf harmonic components of various windings and can also be used to efficiently model the effects of offset machines.

7 Acknowledgment

This work was undertaken as part of a Knowledge Transfer Partnership supported by the Technology Strategy Board, UK.

8 References

- [1] WANG J., XIA Z.P., HOWE D., LONG S.A.: 'Comparative study of 3-phase permanent magnet brushless machines with concentrated, distributed and modular windings'. IET power electronics, machines and drives, Dublin, Ireland, March 2006, pp. 489–493
- [2] COX T., EASTHAM J.F., PROVERBS J.: 'End turn leakage reactance of concentrated modular winding stators', *IEEE Trans. Magn.*, 2008, **44**, (11), pp. 4057–4061
- [3] EASTHAM J.F., COX T., LAI H.C., PROVERBS J., FOSTER A., COLYER S.: 'Electromagnetic launch using novel linear induction machines'. IMarEST engine as a weapon, London, UK, December 2006, pp. 170–179
- [4] EASTHAM J.F., COX T., LEONARD P., PROVERBS J.: 'Linear induction motors with modular winding primaries and wound rotor secondaries', *IEEE Trans. Magn.*, 2008, **44**, (11), pp. 4033–4036
- [5] EASTHAM J.F., COX T., PROVERBS J.: 'Comparison between plate and wound secondaries for linear induction motors with concentrated winding primaries'. SPEEDAM, Ischia, Italy, June 2008, pp. 142–146
- [6] EASTHAM J.F.: 'Improvements in and relating to electromotive machines'. International Patent Application PCT/GB2007/003851, 2007
- [7] EASTHAM J.F., COX T., LAI H.C., PROVERBS J.: 'The use of concentrated windings for offset double stator linear induction motors', *Electromotion*, 2008, **15**, (2), pp. 51–56

[8] EASTHAM J.F., COX T.: 'Transient analysis of offset stator double sided short rotor linear induction motor accelerator'. MAGLEV, San Diego, USA, December 2008

[9] EASTHAM J.F.: 'Improvements in and relating to electromotive machines'. International Patent Application PCT/GB2007/003849, 2007

[10] RODGER D., LAI H.C., LEONARD P.J., HILL-COTTINGHAM R.J.: 'MEGA finite element modelling package', The University of Bath, V6.30, July 2005

[11] LEONARD P.J., RODGER D., LAI H.C., NORTON M., HILL-COTTINGHAM R.J.: 'Coupling FE with power electronics and rotor dynamics of motors'. IEE Seminar on Current Trends in the Use of Finite Elements (FE) in Electromechanical Design and Analysis, January 2000, Ref. 2000/013, pp. 6/1–6/6

[12] ROGER D., LAI H.C., LEONARD P.J.: 'Coupled elements for problems involving movement', *IEEE Trans. Magn.*, 1990, 26, (2), pp. 548–550

9 Appendix: winding analysis

9.1 General three-phase winding

A single general machine winding which consists of a group of coils connected in series is equivalent to a series connection of windings of sinusoidal distribution harmonically related in space. The conductor distribution can be expressed as a Fourier expansion with a zero average term

$$n = \sum_{p=1}^{p=\infty} N_p \cos(p\theta + \varphi_p) \quad (7)$$

It can be taken that the conditions in a machine will be largely unaltered if the conductors and the slots are replaced by patches of infinitely thin conductors positioned on a plane iron surface. The patches of conductors are of the same width and placed in the same positions as the slot openings.

If a slot at θ_s contains N_s conductors and has a slot opening of 2δ then the conductor distribution produced by the slot is given by

$$\bar{N}_p = \frac{1}{\pi} \int_{\theta_s-\delta}^{\theta_s+\delta} \frac{N_s}{2\delta} \varepsilon^{-jp\theta} d\theta, \quad \bar{N}_p = \frac{1}{\pi} \frac{\sin p\delta}{p\delta} N_s \varepsilon^{-jp\theta_s} \quad (8)$$

If the assumption of point conductors is made then

$$\frac{\sin p\delta}{p\delta} \Rightarrow 1 \text{ as } \delta \Rightarrow 0 \quad \text{and} \quad \bar{N}_p = \frac{1}{\pi} N_s \varepsilon^{-jp\theta_s} \quad (9)$$

If the stator has S slots and there are N_{sa} conductors from the a phase in the general s th slot then the a phase winding

distribution is given by

$$\bar{N}_{pa} = \frac{1}{\pi} \sum_{s=1}^{s=S} N_{sa} \varepsilon^{-jp\theta_{sa}} = N_{pa} \varepsilon^{j\phi_{pa}} \quad (10)$$

Similarly

$$\bar{N}_{pb} = N_{pb} \varepsilon^{j\phi_{pb}} \quad \text{and} \quad \bar{N}_{pc} = N_{pc} \varepsilon^{j\phi_{pc}} \quad (11)$$

The winding distributions of a three-phase winding may be represented by positive, negative and zero-phase sequence sets each having three balanced windings. The amplitude and position of the first winding in each set for the p th harmonic is given by

$$\begin{aligned} n_{fp} &= \frac{1}{3} [N_{pa} \varepsilon^{j\phi_{pa}} + N_{pb} \varepsilon^{j(\phi_{pb}+2\pi/3)} + N_{pc} \varepsilon^{j(\phi_{pc}-2\pi/3)}] \\ n_{np} &= \frac{1}{3} [N_{pa} \varepsilon^{j\phi_{pa}} + N_{pb} \varepsilon^{j(\phi_{pb}-2\pi/3)} + N_{pc} \varepsilon^{j\phi_{pc}+2\pi/3}] \\ n_{zp} &= \frac{1}{3} [N_{pa} \varepsilon^{j\phi_{pa}} + N_{pb} \varepsilon^{j\phi_{pb}} + N_{pc} \varepsilon^{j\phi_{pc}}] \end{aligned} \quad (12)$$

As stated previously, when the windings are fed with a balanced set of currents a positive going field is produced by the forward sequence set and a negative going field is produced by the negative sequence set, no field is produced by the zero sequence set. It will be assumed that supply is balanced and therefore that there is no zero sequence field in this Appendix.

9.2 Double-sided offset stator machines

The windings in a double-sided linear machine can be offset to modify the harmonic content of the total field. If \bar{N}_{pa} is the conductor distribution from the a phase winding then the total winding distribution when a second identical phase winding is added at an offset angle of α is

$$\bar{N}_{pat} = N_{pa}(1 + \varepsilon^{-j\alpha p}) = N_{pa} 2\varepsilon^{j\alpha p/2} \cos \alpha p/2 \quad (13)$$

If the second winding is reversed then this becomes

$$\bar{N}_{pat} = N_{pa}(1 - \varepsilon^{-j\alpha p}) = N_{pa} 2j\varepsilon^{j\alpha p/2} \sin \alpha p/2 \quad (14)$$

It follows that the amplitude of the phase sequence distribution from the pair of windings is multiplied by $|\cos \alpha p/2|$ when the offset winding is identical to the first winding and $|\sin \alpha p/2|$ when the offset winding is reversed.

9.3 Three phase nine slot 8/10 modular winding

The layout sequence for the winding is shown in Table 2. The conductor distribution for the leading coil sides of the

'a' phase using (11) is

$$\begin{aligned}\bar{N}_{pa} &= \frac{1}{\pi} \sum_{s=1}^{s=S} N_{sa} \varepsilon^{-j\theta_{sa}} = N_{pa} \varepsilon^{j\phi_{pa}} \\ \bar{N}_{pa} &= \frac{N_{sa}}{\pi} [\varepsilon^{-j0} + \varepsilon^{-j2\pi p/9} + \varepsilon^{-j4\pi p/9}] \\ \bar{N}_{pa} &= \frac{N_{sa}}{\pi} \varepsilon^{-j2\pi p/9} [\varepsilon^{j2\pi p/9} + \varepsilon^{-j2\pi p/9}] - \varepsilon^{-j2\pi p/9} \\ \bar{N}_{pa} &= \frac{N_{sa}}{\pi} \varepsilon^{-j2\pi p/9} [2 \cos 2\pi p/9 - 1]\end{aligned}\quad (15)$$

Then since the lagging coil sides are a reverse repeat of this pattern offset by a coil pitch $\sin 2\pi/9$ it follows that total \bar{N}_{pa} is equal to (15) multiplied by $\sin \pi p/9$. The winding factor can be defined as the modulus of the winding distribution divided by the maximum possible winding amplitude N_{SA}/π , giving

$$\bar{k}_{wp} = |[2 \cos 2\pi p/9 - 1] \sin \pi p/9| \quad (16)$$

The equivalent expressions for the other two phases may be found by an origin shift hence

$$\bar{N}_{pa} = N_p \text{ then } \bar{N}_{pb} = N_p \varepsilon^{-2\pi p/3} \text{ and } \bar{N}_{pc} = N_p \varepsilon^{2\pi p/3} \quad (17)$$

Using (12) the phase sequence winding sets can now be found

$$n_{fp} = \frac{N_p}{3} [1 + \varepsilon^{j(-2\pi p/3+2\pi/3)} + \varepsilon^{j(2\pi p/3-2\pi/3)}] \quad (18)$$

it follows that $n_{fp} = N_p$ if $p = 1, 4, 7 \dots$ and is zero for all other values

$$n_{np} = \frac{N_p}{3} [1 + \varepsilon^{j(-2\pi p/3-2\pi/3)} + \varepsilon^{j(2\pi p/3+2\pi/3)}] \quad (19)$$

it follows that $n_{np} = N_p$ if $p = 2, 5, 8 \dots$ and is zero for all other values

When the winding is fed with a balanced set of three-phase currents, positive going waves are produced at $p = 1, 4, 7, \dots$ and negative going waves are produced when $p = 2, 5, 8, \dots$

When this winding is used to construct an offset stator double-sided machine the total winding distribution for the two sides can be found using (13) if the second winding is the same as the first or (14) if it is reversed.